Online measurements of fluoride ions in proton exchange membrane water electrolysis through Ion Chromatography

Paolo Marocco[a], Kyrre Sundseth[b], Thor Aarhaug[b], Andrea Lanzini[a], Massimo Santarelli[a], Alejandro Oyarce Barnett[b,c], Magnus Thomassen[b]*

[a]Department of Energy, Politecnico di Torino, Torino, Italy

[b]New Energy Solutions Department, SINTEF Industry, Trondheim, Norway

[c]Department of Energy and Process Engineering, Norwegian University of Science and Technology, NO-7491 Trondheim, Norway

*Corresponding author: paolo.marocco@polito.it

Abstract

This work investigates the online monitoring of fluoride ion concentration in proton exchange membrane water electrolysers (PEMWE) effluent water using an automated ion chromatography (IC) setup. Prototype catalyst coated membranes (CCMs) with different thicknesses have been tested and fluoride measurements under different operating conditions at both single cell and stack level have been carried out. The study reports the impact of both current density and temperature on the cathodic fluoride concentrations showing a maximum at low current densities, at around 0.4 A/cm^2 for the single cells, and at 0.2-0.4 A/cm^2 for the short stack. It is also reported that higher PEMWE working

temperature has an adverse effect on the membrane stability, resulting in a significant increase of the fluoride release at the cathode outlet. Noticeably, CCMs with reduced membrane thickness exhibited lower values of area-specific fluoride release rates with respect to thicker CCMs. Finally, the study also reports that fluoride concentrations and water conductivity are very well correlated, displaying a linear correlation. This new finding could represent a low cost and straightforward method to obtain quantitative information about membrane degradation rates in larger commercial PEMWE systems.

Keywords

Hydrogen, PEM electrolysis, fluoride release, membrane chemical degradation, ion chromatography, thin perfluorinated sulfonic acid membranes.

1. Introduction

The perfluorinated sulfonic acid (PFSA) membrane is one of the components in proton exchange membrane water electrolysers (PEMWE) most susceptible to degradation and failure. Chemical degradation caused by radical attack and subsequent membrane thinning and loss of functional groups is indeed one of the main degradation mechanisms known for PEMWEs. As thick membranes in the range of 180 µm commonly are used in PEMWE, thinner PFSA membranes represent a promising way to decrease both energy use and investment cost in the PEMWE since reduced voltage losses and thus higher current densities can be achieved. However, this strategy is challenging as it can result in accelerated chemical degradation due to increased gas crossover rates.

In a PEM electrolyzer, the membrane is required to separate the reaction products (i.e., hydrogen and oxygen) and to efficiently transport protons from anode to cathode. The

membrane thus needs to have good proton conductivity, good gas crossover resistance and excellent chemical, thermal and mechanical stability [1]. Perfluorinated sulfonic acid (PFSA)-based membranes are most commonly used because of their high stability and proton conductivity. However, the PFSA membrane is stated to be one of the weakest components in a PEM electrolyser for long term performance [2]. Stucki *et al.* [3] showed the electrolyser failure to be attributed to the degradation process of the Nafion-based membrane. Their system had to be shut down for safety reasons after detecting excessive levels of hydrogen in oxygen. The reason was a substantial thinning of the membranes in the stack with consequent increase of the gas cross-permeation effects. Chemical degradation resulting in membrane thinning was also revealed to be an important contributor to PEM cell failure by Grigoriev *et al.* [4]**.**

During the electrolysis process, oxygen crossover occurs from the anode to the cathode side due to diffusive and convective phenomena [5][6]. In the presence of platinum, as in the case of PEMWE cathode catalyst layers, hydrogen peroxide can be generated according to the following reaction:

$$O_2 + 2H^+ + 2e^- \leftrightarrow H_2O_2 \qquad \text{(R1)}$$

Although working conditions in PEMWE are different from those in fuel cell (FC) operation, degradation mechanisms during electrolysis can be deduced from PEMFC research since the adopted membrane materials are generally the same. In the presence of metal ions, hydrogen peroxide can lead to the formation of radicals, which are responsible for the chemical attack to the membrane. Certain transitional metal ions, such as iron and copper, were found to be the most dangerous regarding the acceleration of the degradation process [7]. In particular, Fe^{2+} was shown to have the highest impact on the chemical degradation rate [8][9]. Metallic cation impurities mainly originate from feed water, corrosion of pipes and stack components and fabrication processes of the CCM [2][10]. Fenton's reaction

mechanism in the presence of ferrous iron allows to decompose hydrogen peroxide into highly reactive hydroxyl radicals (OH^*):

$$H_2O_2 + Fe^{2+} \rightarrow Fe^{3+} + OH^- + OH^* \quad \text{(R2)}$$

The so formed radicals are responsible for attacking the membrane with consequent membrane thinning and release of fluoride ions. It is generally accepted that the degradation process occurs via an unzipping mechanism involving carboxylic acid end groups (-COOH) [11]. Overall, each carboxylic acid end group reacts with two hydroxyl radicals leading to the release of one CF_2 unit in the form of one CO_2 molecule and two HF molecules:

$$\text{-}(CF_2)_j\text{-}COOH + 2OH^* \rightarrow \text{-}(CF_2)_{j-1}\text{-}COOH + CO_2 + 2HF \quad \text{(R3)}$$

Carboxylic acid end group units are usually located at the end of the main chain of the fresh Nafion-based structure. However, more chemically stabilized membrane typologies have recently been developed, reducing the terminal -COOH groups to negligible levels [12]. Carboxylic acid end groups can also be generated within the membrane through different pathways occurring during the electrolyser operation. One option is that -COOH originates from the weak non-perfluorinated polymer end groups after reacting with hydroxyl radicals. Another mechanism suggests the Nafion side chain to be the -COOH source [13][14]. Nevertheless, once the –COOH unit is formed, the degradation process propagates according to the unzipping reaction (i.e., reaction 3) with subsequent release of HF molecules [15].

The rate of chemical degradation may thus be determined by measuring the fluoride ion content (from HF dissociation in water) at the PEM electrolyser exhaust. Baldwin *et al.* [16] reported a correlation between the emission of fluoride ions and the PEM cell lifetime. Since then, the fluoride release rate (FRR) monitoring has become a reliable diagnostic tool to assess the chemical durability in the PEMFC field [17]. However, studies dealing with FRR

measurements in PEMWE operation are few [8][18][19][20][21]. Fluoride ion selective electrode (ISE) and ion chromatography (IC) have been both shown to be sensitive and accurate for fluoride ion detection, with the former more commonly employed since it is simpler and more straightforward. In addition, IC has the advantage of being able to simultaneously measure fluoride and other degradation products. Both techniques can potentially be automated for online monitoring of FRR in the PEM device's effluent water [22].

Fouda-Onana *et al.* [18] investigated the membrane degradation using two different ageing protocols at 60°C and 80°C, respectively. Chemical degradation was analyzed by regularly collecting exhaust water at the anode and cathode side and subsequently measuring the FRR by means of a fluoride ISE. Fluoride was mainly found on the cathode side, which is in accordance with the mechanism of membrane degradation caused by radical attack. With a similar set-up, Chandesris *et al.* [19] confirmed that most of the chemical degradation occurs at the cathode side and showed temperature to have a strong influence on the degradation rate with a peak of FRR at a current density of around 0.2-0.4 A/cm^2. A 1D PEMWE model was also developed to analyze the influence of both temperature and current density and study the time evolution of the membrane thickness. The model developed by Chandesris *et al.* [19] was later improved by Frensch *et al.* [20], who analyzed the influence of iron and hydrogen peroxide and performed ex-situ tests to fit the model parameters. Results showed that H_2O_2 acts as required precursor, while iron impurities catalyze the reaction considerably. In the framework of the FCH-JU project NOVEL [21], accelerated stress tests (ASTs) were carried out and their impact on the membrane chemical durability was also monitored by means of FRR measurements using fluoride ISE. Ex-situ SEM images were performed to compute the membrane thinning rate. Low current values and high temperatures were found to speed up the membrane chemical attack. A long-term durability

test at stack level was also performed showing a gas purity degradation rate of H_2 in O_2 leading to a stack lifetime of approximately 42,000 hours. According to the published reports, monitoring the fluoride amount in the exhaust water on the cathode side seems to be a reliable indicator of the membrane degradation. Moreover, CCM lifetime can be estimated based on FRR measurement (the loss of around 10% of the overall fluoride inventory is usually considered as a criterion for the CCM end of life [8][15]).

The aim of this study is to perform automated online measurements of FRR from a single cell and short-stack PEM electrolyser using ion chromatography and to study the influence of operating conditions such as current density and temperature. To our knowledge, no studies have been published referring to online automated monitoring of fluoride concentration during water electrolysis using IC. Another objective of the study is to measure the FRR from thinner membranes. Thinner membranes allow the operation at higher current densities and can contribute to reduce the investment cost for PEMWE due to a higher rate of hydrogen production per unit cell area of the electrolyser [23]. However, the increased crossover of gases due to the reduced membrane thickness may not only become potentially dangerous if the hydrogen concentration reaches 4%, but it may negatively affect CCM degradation rates. The present work will give a first insight into membrane chemical degradation referring also to thinner membranes; similar studies have not been found for PEM electrolysis.

2. Experimental

2.1 Catalyst coated membranes (CCMs) and cells

Two different catalyst coated membranes (CCM) based on Nafion 117 and Nafion 212 with a thickness of 183 and 50.8 micrometers, respectively, have been investigated. The active area of the CCMs is 25 cm^2 using an Ir-based anode catalyst layer (CL) and Pt-based

cathode CL, with loadings of approximately 2 mg/cm^2 Ir and 1 mg/cm^2 Pt. Detailed specifications of the catalyst layers, e.g. catalyst type, ionomer type and ionomer loading can unfortunately not be disclosed. The commercial CCM producer required to be anonymous in this publication. More importantly for this study, both the Nafion 117 and Nafion 212 CCMs have the same catalyst type, loading, ionomer type and loading and can directly be compared.

Flow fields at the anode and cathode side are both made of titanium. Platinum (Pt)-coated titanium is used for the anode and cathode porous transport layers (PTL). Titanium (Ti) is required because of its high stability to corrosion. The Pt protective coating over the Ti-based PTLs is usually employed in industrial PEMWE applications and applied to avoid titanium passivation that could result in high interfacial contact resistances [2]. Pressure paper tests were performed to have a good homogeneous pressure distribution across the active area. A clamping torque of 15 Nm/bolt was found to be optimal for the cell assembly.

The single cell PEM electrolyser was subjected to a hydration and a break-in procedure. The hydration procedure included circulating 0.2 LPM of DI-water at both anode and cathode overnight at 40^{o}C at half of the final clamping torque (7.5 Nm/bolt). The cell is afterwards clamped to 15 Nm/bolt before starting the break-in procedure. This procedure involves polarising the electrolyser in steps of 0.1 A/cm^2 for 5 min until reaching 2 V for 60^{o}C, 70^{o}C and 80^{o}C. The electrolyser is then left at open circuit voltage over night at 40^{o}C with recirculation of 0.2 LPM of DI-water at both anode and cathode. After the initial membrane hydration and break-in procedure, tested CCMs have been characterized in terms of polarization curves under various operating conditions, i.e., temperature (60-80°C range) and cathode side pressure (0-4 barg range). Polarization curves measurements were carried out following the testing procedure reported by Malkow *et al.* [24]. Tests were

performed under galvanostatic control and aborted when reaching a cut-off voltage of 2 V or a current density upper limit of 4 A/cm^2.

Measurements made at stack level were performed to validate the IC measurement methodology for larger cells. The PEM water electrolysis short stack was purchased from Proton Onsite and all electrolyser components, e.g. CCM, PTLs, BPPs are proprietary information and were not disclosed. The stack is composed of 10 cells and is designed to operate in the temperature range 35-60°C (with 50°C as nominal temperature) and with a maximum current of 1.86 A/cm^2.

2.2 Electrolyser test stations and set-up

Commercial PEMWE test stations from Greenlight Innovation installed at the Norwegian Fuel Cell and Hydrogen Center were used in all the measurements [25]. For the single cell testing a Greenlight E40 test station with a power supply with a maximum of 100 A was used. For the stack testing a Greenlight E100 with a power supply with a maximum of 500 A was used. Both test stations have anode and cathode water circuits, where both the anode and cathode circuit are designed to work with water recirculation. A schematic of the cathode circuit is shown in Figure 1a (the anode one is analogous). The water flow exiting the cathode outlet is sent to the H_2 separator and then recirculated by a pump. The pump controls the flow using the signal from a mass flow controller located at the electrolyser inlet. As shown in Figure 1a, a portion of the recirculated water enters a mixed bed filled polisher containing a ion exchange resin (Aldex MB-1 (SC)). The water ratio entering the polisher is controlled by a needle valve.The functionality of the resin is very important in commercial PEMWEs, as highly purified water is required to minimize metallic cation impurities. Cationic species can lead to a reduction of the ionic conductivity of the membrane [26][27][28], contribute to catalyst poisoning [2][27] and enhance the chemical degradation process of

the membrane [18]. A heat exchanger for cooling purposes and an electric heater are also present for the electrolyser thermal management by acting on the temperature of the recirculated water flow. Water conductivity was measured by means of ConduMax W CLS 13 conductivity sensors. The percentage level of hydrogen in oxygen was monitored with a K1550 series H_2 analyser. An anodic hydrogen content of 2 vol.%, which corresponds to around 50% of the lower explosion limit (LEL), was set as upper limit, above which the machine is automatically stopped for safety precautions.

All IC measurements of fluoride ion concentration were carried out on the cathode side of the PEM electrolysers. Fluoride release has been shown to be far larger at the cathode than at the anode [18][19][21], which is in accordance with the hypothesis of membrane degradation occurring mainly in the cathode side region. Platinum, which catalyses the H_2O_2 formation reaction (i.e., reaction 1), is in fact mainly found within the cathode CL of the PEM cell. The low cathodic potential also favours reaction 1, whose equilibrium potential is 0.695 V vs. SHE [29][30]. As graphically represented in Figure 1a, a fraction of the water flow exiting the cathode channel was periodically delivered to the IC for fluoride evaluation in automated way. The online IC sampling was designed also for the cathode inlet. In the cathode circuit, a water loop is present, and the recirculated water is fractioned between the electrolyser and the resin, which are positioned in parallel. Fluoride ions can thus be present in the portion of the recirculated water flow entering the cathode channel. For a correct quantification of the FRR the fluoride ions concentration at the cathode inlet was also measured.

a)

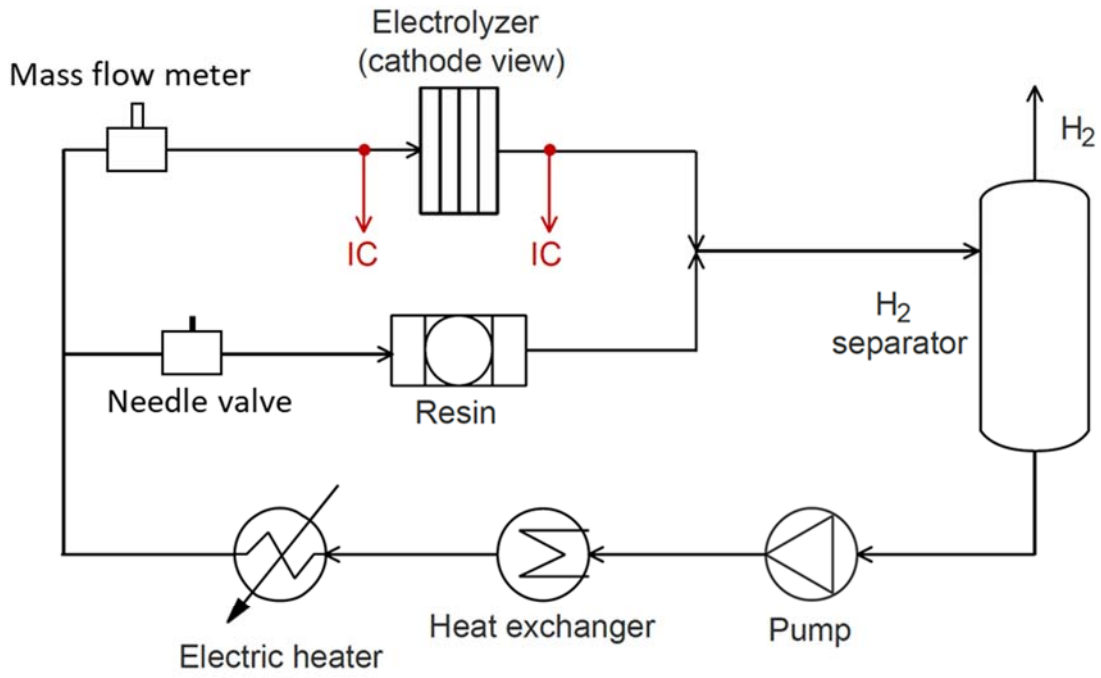
Mass flow meter
Electrolyzer
(cathode view)
IC
IC
H_2
H_2
separator
Needle valve
Resin
Heat exchanger
Pump
Electric heater

b)

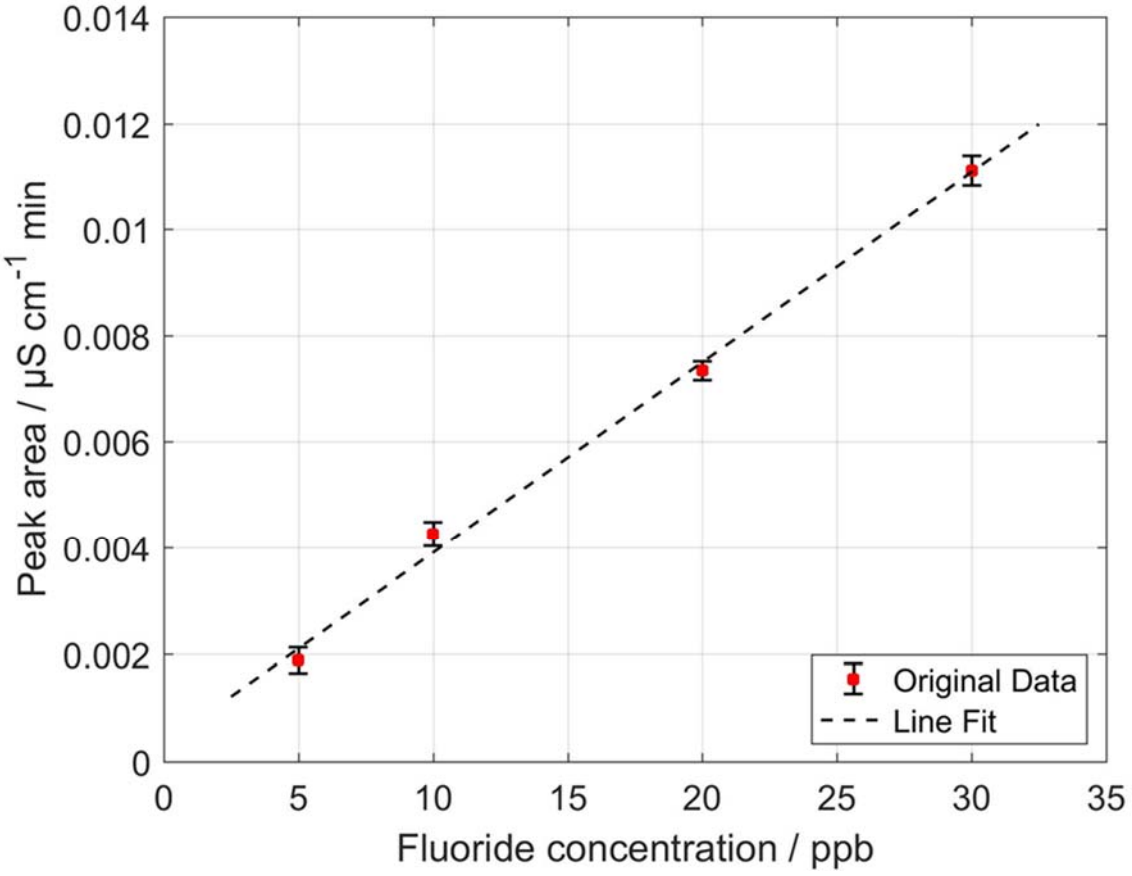
Peak area / µS cm^{-1} min
Fluoride concentration / ppb
0.014
0.012
0.01
0.008
0.006
0.004
0.002
0
0
5
10
15
20
25
30
35
Original Data
Line Fit

Figure 1. (a) *Schematic of the cathode loop for both the single cell and stack test stations, including the electrolyser cells, resin polisher, gas separator, pump, heat exchanger and heater. The anode loop is analogue to the cathode loop in both test stations.* ***(b)*** *Example of standard sample measurement and related calibration curve.*

2.3 Fluoride measurements

An 850 Professional IC – Anion – MCS - Prep 2 device was used to perform automated online ion chromatographic determination of fluoride ion concentration at the cathode outlet and inlet (Figure 1a). In a typical IC instrument, the eluent is fed through a high-pressure pump. A sample of the mixture to be analysed, i.e., the analyte, is added to the eluent flow in the injector component. The eluent+analyte is then sent to the chromatographic column (Molsieve 15 cm) where the separation of the analyte components occurs. After separation, a suppression step is performed to decrease the eluent background conductivity and enhance the conductivity of the sample ions. Finally, a conductivity detector is used for the analyte quantification process.

A sequential suppression was adopted to reduce the background conductivity to a minimum: chemical suppression through the Metrohm suppressor module (MSM) followed by CO_2 suppression with the Metrohm CO_2 suppressor (MCS). The sample degasser unit was also added to remove potential gas bubbles and dissolved hydrogen from the sample to be analysed. The eluent consists of a mixture of Na_2CO_3 (0.339 g/L) and $NaHCO_3$ (0.084 g/L) dissolved in DI water. Its flow rate was set to 0.7 mL/min. Concerning the MSM, DI H_2O was used as rinsing solution whereas a solution of H_2SO_4 in DI H_2O (3 mL/L) acts as regenerator. The above described IC set-up allows to obtain an automated online IC measurement every approximately 24 minutes: around 5 minutes for the sample rinsing time plus 19 minutes of

recording time (to allow all the analytes to cross the column). The sample rinsing time was chosen to prevent contamination of samples by the previous sample.

IC calibration is required to convert peak areas from the measured samples into concentrations. By diluting a multi-element IC anion standard solution (Multi Anion Standard 1 for IC from Sigma-Aldrich), standard samples with different known fluoride ion concentration were made and used for the calibration of the ion chromatography instrument. The different peak area values were then plotted versus the fluoride ion concentration and a calibration curve, as the one shown in Figure 1b, was thus obtained by linear fitting. The calibration process was performed periodically to guarantee accuracy of results.

Current sensitivity tests were carried out to investigate the effect of current on the release of fluoride ions. The influence of temperature was also considered. Each operating condition was maintained for a certain time interval (approximately 6 hours) to reach stabilization in IC fluoride measurements. Besides the continuous acquisition of fluoride concentration values over the test period, other PEMWE cell parameters were also monitored and logged, e.g., cell voltage, current, anode/cathode inlet/outlet temperature and pressure, conductivity of the stream in the anode/cathode circuit, mass flow rate of H_2 production and H_2 in O_2 signal at the anode.

3. Results and discussion

3.1 Single cell PEMWE performance

The performance of the three tested CCMs at single cell level was investigated by recording a set of polarization curves. For the sake of comparison, Figure 2 shows the polarization curve measurements at 60°C (a) and at 80°C (b) and ambient pressure at beginning of life (BOL), just after the break-in procedure for the CCMs.

As can be observed from Figure 2a, when working at 60°C, the performance of the two Nafion 117-based membranes are quite similar, with a current density slightly higher than 1.5 A/cm^2 at the cut-off voltage of 2 V. The Ohmic resistance of the cells was estimated from the slopes of the polarisation curves, resulting in 254 mΩ cm^2 and 266 mΩ cm^2, for the two N117a and N117b CCMs, respectively. Due to the lower Ohmic resistance (123 mΩ cm^2) resulting from thinner membrane, the performance of the Nafion 212-based CCM is drastically improved: at 2 V, the corresponding current density is around 3.7 A/cm^2, which is more than double the one of Nafion 117 CCMs.

Polarization curves at 80 °C are displayed in Figure 2b , showing an enhancement of the cell performance compared to 60 °C. The better performance is partially associated to improved OER and HER kinetics, as well as lower Ohmic resistances at higher temperatures, as water uptake and proton conductivity is increased. The Ohmic resistance was 219 mΩ cm^2 and 226 mΩ cm^2, for the N117a and N117b CCMs, respectively, while the thinner N212 based CCM showed a cell resistance of 113 mΩ cm^2. Current density for the Nafion 117 membranes increases from around 1.5 A/cm^2 at 60°C to approximately 2 A/cm^2 at 80°C at the cut-off voltage of 2 V. Moreover, the thinner membrane is able to reach current densities as high as 4 A/cm^2 at around 1.9 V. Only slightly higher voltages in the activation region were observed when changing the cathode pressure from 0 to 4 barg (not shown).

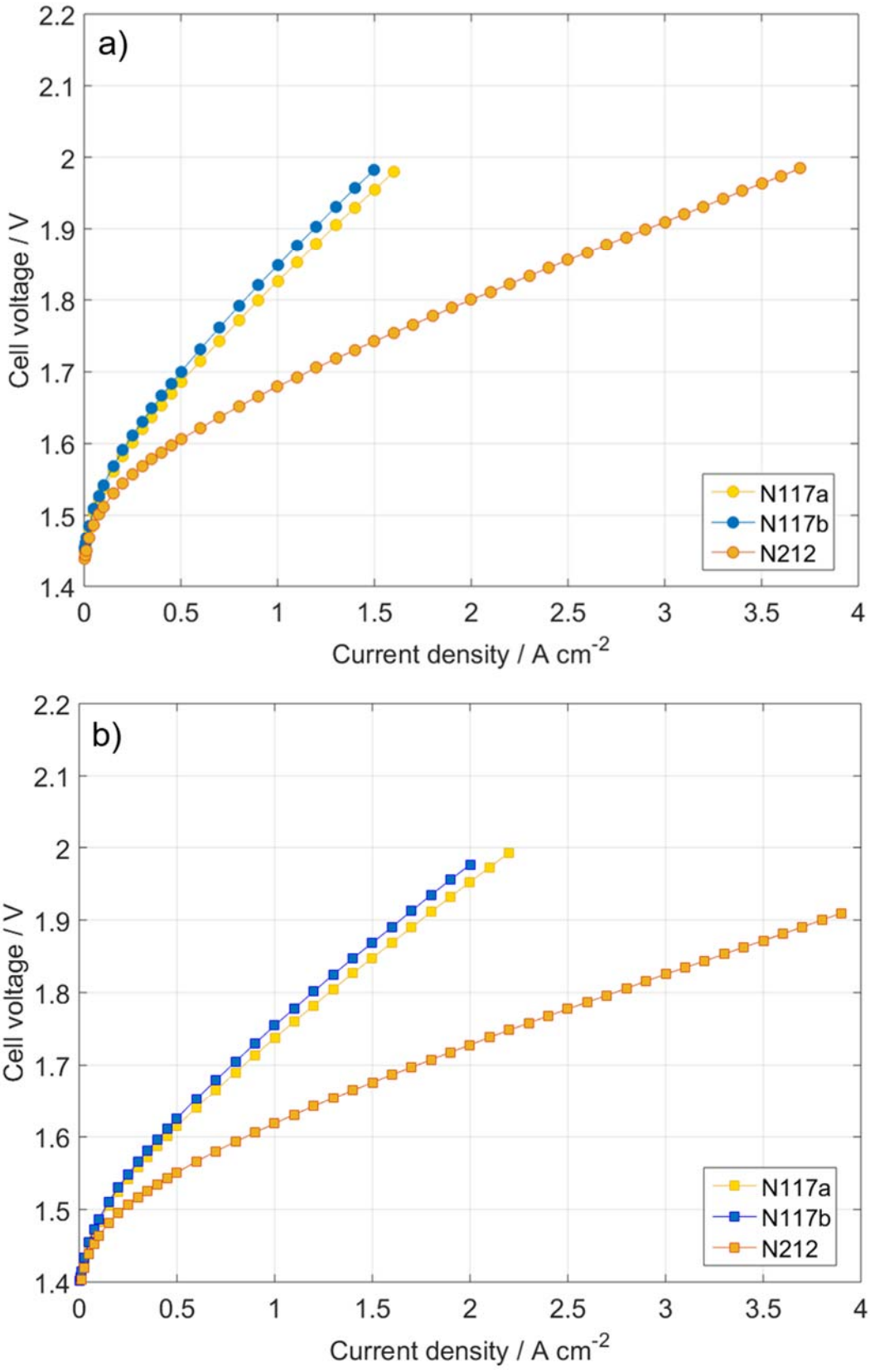

***Figure 2**. BOL polarization curves of CCMs at ambient pressure, 0.2 LPM of water at the anode/cathode inlet and temperature of 60°C **(a)** and 80°C **(b)**.*

3.2 Fluoride concentration at single cell cathode outlet

Figure 3a shows the effect of the operating current density on the fluoride concentration at the cathode outlet stream for the first tested Nafion 117-based CCM (i.e. Nafion 117a). The behaviour of the water conductivity at the cathode is also shown in the same graph. Due to the continuous online fluoride monitoring, it was possible to detect transients in fluoride emission. The current range between 0.2 to 2 A/cm^2 was measured with steps of 0.2 A/cm^2. Each current density value was set constant for around 6 hours, before moving to the subsequent value. The entire test was carried out at a constant temperature of 60 °C and with a cathode recirculated water flow rate of 0.15 LPM. A maximum in the fluoride ion concentration can be observed at a current density of 0.4 A/cm^2 with a gradual reduction with increased current density. It is also evident that there is a similar trend for the fluoride concentration and cathode conductivity profiles.

Similarly, the current density influence was analyzed for the other Nafion 117 CCM, i.e., Nafion 117b (Figure 3b and 3c) and the thinner Nafion 212 CCM (Figure 4a and 4b). The effect of temperature was also investigated by performing current sensitivity tests at two different temperatures, 60 and 80°C. As it can be seen from Figure 3b and 3c, a fluoride peak at quite low current densities, at around 0.4-0.6 A/cm^2, is evident for both the tests at 60 and 80 °C. During the operation at 80°C (i.e., Figure 3c), the test was stopped after around 12 hours because of an unexpected external event and started again from the 0.6 A/cm^2 case. Higher values of fluoride ions are observed when the temperature is changed from 60 to 80°C. The measured fluoride concentration at 80°C was found to be around five-six times higher than the one at 60°C for all the considered values of current density. Figure 3b and 3c also show both the anodic and cathodic water conductivity values along the test.

The change in the value of the conductivity at the anode side by varying the current density is very low, even when operating at high temperatures as clearly displayed in Figure 3c.

The experimentally observed trends are in accordance with results obtained by Fouda-Onana *et al.* [18] and Chandesris *et al.* [19] on Nafion 117-based membranes. The fluoride release and hence the degradation of the membrane is enhanced when increasing current density and reaches a maximum at around 0.4 A/cm^2, after which the fluoride release starts to decrease. Chandesris *et al.* [19] developed a PEMWE model incorporating chemical degradation of the membrane. They explained the decrease in fluoride release at higher current densities by the reduced molar percentage of oxygen at the cathode side, Thus, the peroxide formation, which depends on the oxygen concentration (reaction 1), is slowed down with a consequent reduction in the formation of free radicals. Reactions leading to membrane attack (i.e., reaction 3) and the following reaction involving hydrogen peroxide (reaction 4) were found to be the main consumption reactions of hydroxyl radicals (OH*).

$$OH^* + H_2O_2 \rightarrow OOH^* + H_2O \qquad \text{(R4)}$$

The competition between reaction 3 and reaction 4 was assumed to be the main reason for the observed fluoride release peak at low current. Specifically, in the low current density range, the high anodic oxygen molar fraction favors the formation of hydrogen peroxide through reaction 1. Due to the high H_2O_2 concentration, reaction 4 is thus enhanced and, below a certain current, becomes predominant over the membrane chemical attack reactions (reaction 3), leading to a decrease in the degradation rate (i.e., lower fluoride emission).

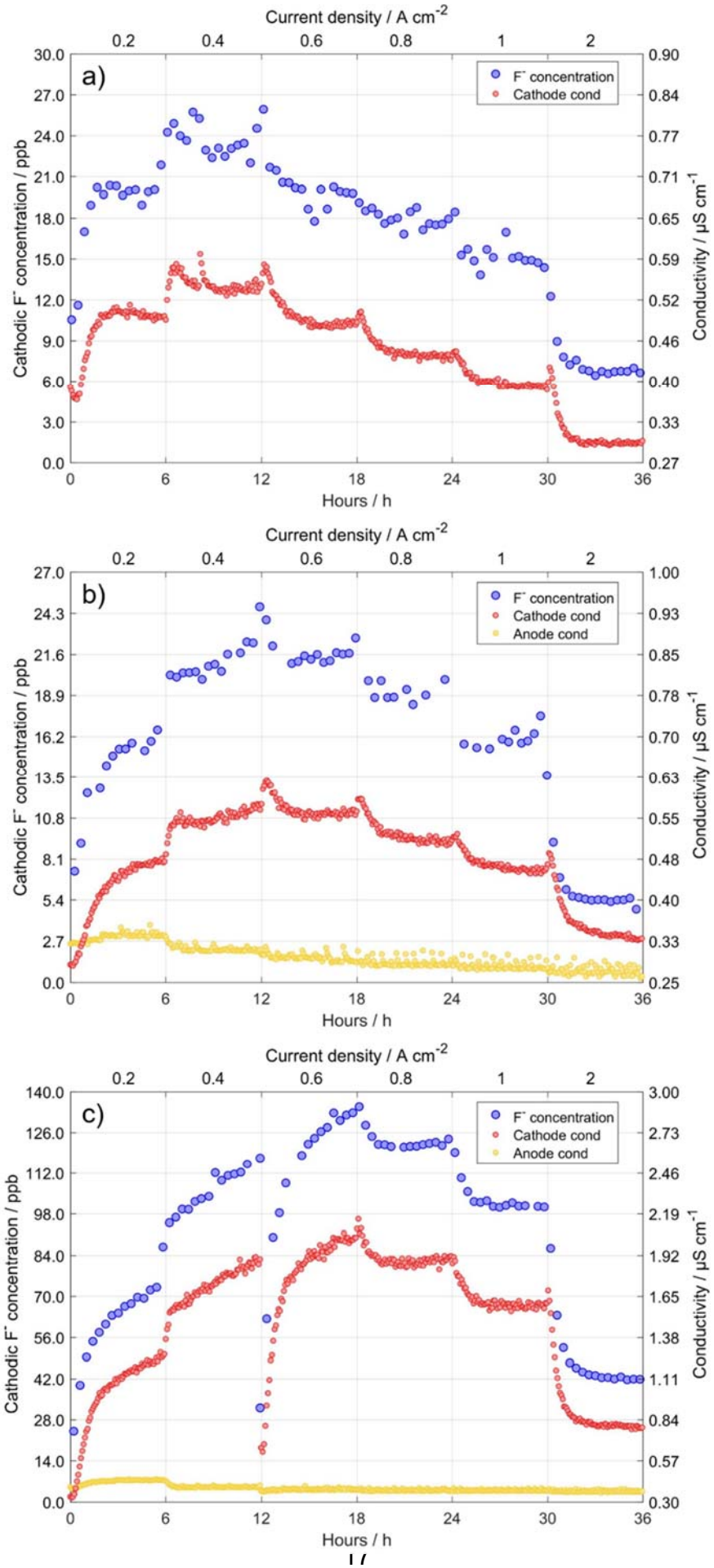
a)
b)
c)
Current density / A cm-2
0.2
0.4
0.6
0.8
1
2
F- concentration
Cathode cond
Anode cond
Cathodic F- concentration / ppb
Conductivity / µS cm-1
Hours / h
0
6
12
18
24
30
36

Figure 3. *Nafion 117-based CCM tests: Effect of current density on the fluoride concentration at the cathode outlet and on the cathode water conductivity (with 0.15 LPM recirculated water at the cathode side).* ***(a)*** *Current sensitivity at 60°C for the Nafion 117a CCM,* ***(b)*** *current sensitivity at 60°C for the Nafion 117b CCM and* ***(c)*** *current sensitivity at 80°C for the Nafion 117b CCM.*

Figure 4 shows the fluoride concentration and water conductivity for the Nafion 212 CCM. An additional 6 hour-test was also performed at 3 A/cm^2 to investigate the fluoride release at even higher current densities. The Nafion 212 shows a much lower fluoride release compared to the two Nafion 117 CCMs, with a fluoride concentration peak at 60 °C of around 6.3 ppb in comparison to the 24 ppb of the Nafion 117. The fluoride peak for the thinner CCM is shifted to slightly higher currents densities compared to the thicker CCMs. Referring to the 60°C case, the fluoride concentration reaches its maximum when operating at 0.6 A/cm^2 (Figure 4a). The fluoride peak also shifts with increasing temperature to a value of around 0.8 A/cm^2 when working at 80°C (Figure 4b). A two to three-fold increase in fluoride concentration was detected for the Nafion 212 membrane in the 0.2-3 A/cm^2 range when moving from 60 to 80°C. Likewise to the other tested CCMs, the cathodic fluoride concentration and water conductivity present a similar behavior as a function of current density and temperature. A very low variation of the anodic water conductivity value by changing the current density can be observed as well.

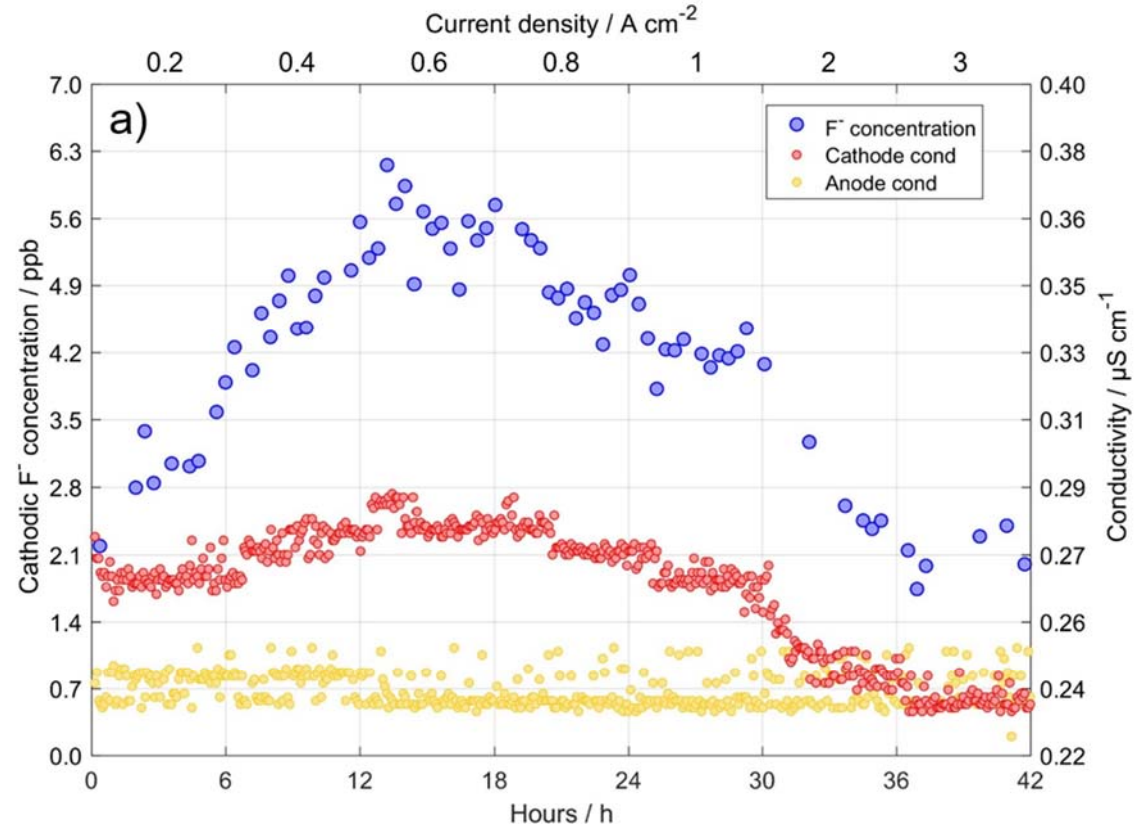
a)
Current density / A cm-2
0.2
0.4
0.6
0.8
1
2
3
F- concentration
Cathode cond
Anode cond
Cathodic F- concentration / ppb
Conductivity / µS cm-1
Hours / h
0
6
12
18
24
30
36
42

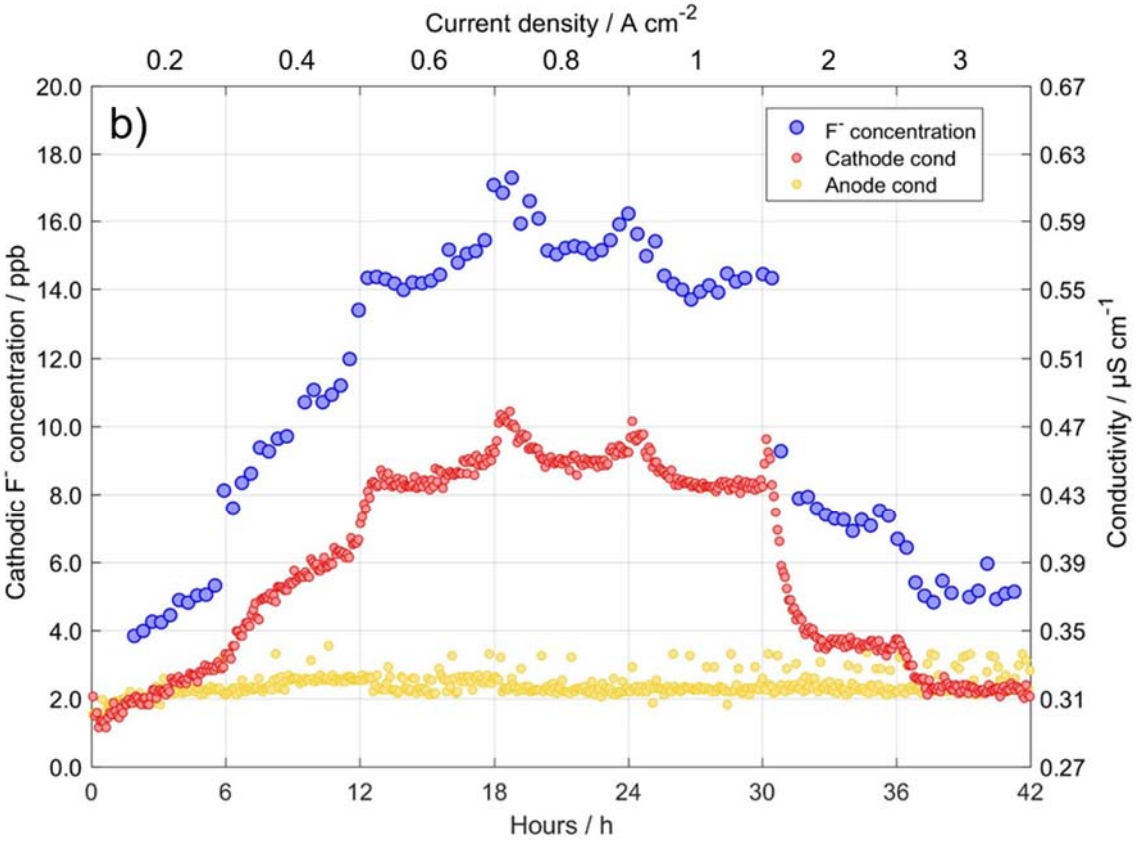
b)
Current density / A cm-2
0.2
0.4
0.6
0.8
1
2
3
F- concentration
Cathode cond
Anode cond
Cathodic F- concentration / ppb
Conductivity / µS cm-1
Hours / h
0
6
12
18
24
30
36
42

Figure 4. *Current sensitivity at 60°C* ***(a)*** *and 80°C* ***(b)*** *for the Nafion 212 CCM with 0.15 LPM recirculated water at the cathode side: effect of current density on the fluoride concentration at the cathode outlet and on the cathode water conductivity.*

3.3 Fluoride-conductivity correlation

Figure 5 shows fluoride IC measurements plotted against measured conductivity to investigate the correlations between the two variables. All results from the current sensitivity tests at 60 and 80°C of the three CCMs have been reported. A good linear correlation can be seen with a R-squared value of approximately 0.949 at 60°C (Figure 5a) and 0.998 at 80°C (Figure 5b).

A linear correlation between water conductivity and F^- ions concentration has been reported earlier by Pozio *et al.* [31], but referring to the PEM fuel cell field. Water conductivity depends mainly on H^+ ions, whose release can be justified in the presence of anions to guarantee water charge neutrality [31]. It can be deduced the concomitant occurrence of F^- and H^+ ions in the water flow as also showed by Healy *et al*. [32], where a relationship between fluoride concentration in fuel cell exhaust water (in terms of pF, i.e., $-\log_{10}[F^-]$) and pH was demonstrated. The measured fluoride is thus released primarily in the form of HF, which is a weak acid (pK_a equal to 3.2) and will dissociate into H^+ and F^- ions. This is in accordance with a degradation mechanism involving radical attack on fluorinated backbones with consequent HF production, as for example reported by the unzipping degradation process globally described by reaction 3. The measured conductivity values are also in line with HF conductivity data estimated from the theory of ionic solutions [33], thus confirming HF is the main product released by the membrane and affecting the water conductivity.

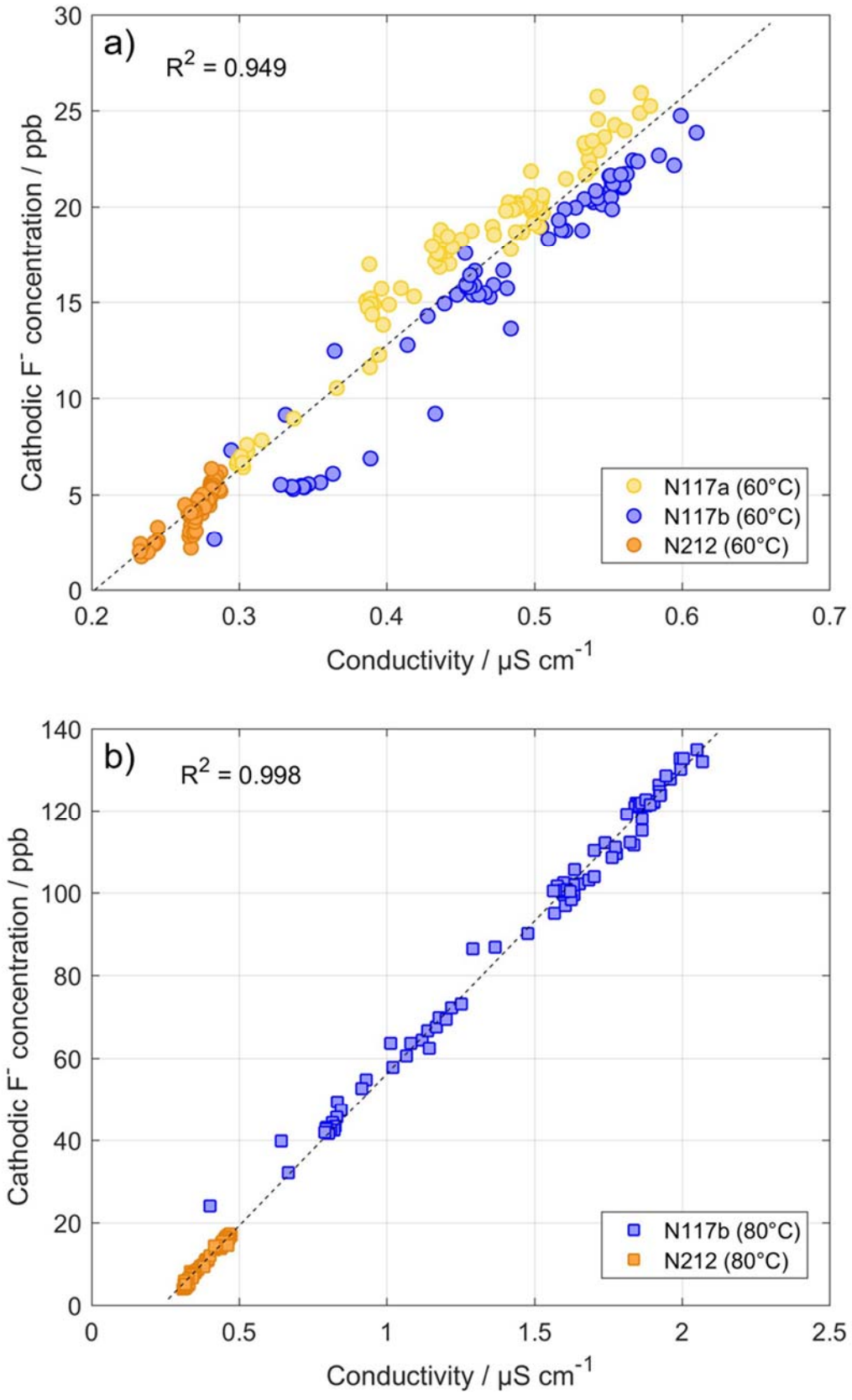

Figure 5. *Fluoride concentration at the cathode outlet vs. water conductivity in the cathode circuit for all three CCM characterized in this study at 60 °C* ***(a)*** *and 80 °C* ***(b)***

By reasonably supposing the existence of a correlation between fluoride concentration and conductivity also on the anode side, it can be deduced that the FRR occurs mainly on the cathode side, which is in line with other experimental observations [18][19] and the commonly accepted CCM chemical degradation mechanism.

3.4 Normalisation of FRR

The cathodic area specific fluoride release rate (FRR_A), i.e., the amount of fluoride which is released in the cathode channel per unit of CCM active area and per unit of time, is derived according to the following relationship:

$$FRR_A = \frac{\left(ppb_{F,cat,outlet} \cdot \dot{V}_{H_2O,cat,outlet} - ppb_{F,cat,inlet} \cdot \dot{V}_{H_2O,cat,inlet}\right) \cdot 60}{A_{cell}} \quad \text{Eq. 1}$$

Where FRR_A is the area specific FRR (in µg $h^{-1}cm^{-2}$), $ppb_{F,cat,outlet/inlet}$ (in parts per billion) corresponds to the cathodic fluoride concentration at the cathode outlet/inlet, $\dot{V}_{H_2O,cat,outlet/inlet}$ (in LPM) represents the volume flow rate of water at the cathode outlet/inlet and A_{cell} (in cm^2) is the active area of the PEMWE CCM.

As reported in the above FRR formula, the amount of F^- ions at the inlet of the cathode needs to be measured as well for a proper quantification of the FRR. Fluoride ions are in fact also found at the cell inlet since, as previously stressed in the Experimental section, the cathode circuit is designed to operate with water recirculation and with the cell and the resin unit arranged in parallel as commonly done for commercial electrolyser systems. It was found that the inlet fluoride concentration (i.e., $ppb_{F,cat,inlet}$) was at all times 83% of the

cathode outlet when working with a recirculated water feed flow rate of 0.15 LPM. This value was then used to compute the net fluoride released by the CCM.

The volume flow rate of water exiting the cathode channel is:

$$\dot{V}_{H_2O,cat,outlet} = \dot{V}_{H_2O,cat,inlet} + \dot{V}_{H_2O,cross} \quad \text{Eq. 2}$$

Where $\dot{V}_{H_2O,cross}$ stands for the amount of water flowing through the PEM membrane. It is mainly due to the electro-osmotic drag process, the water concentration gradient and the pressure gradient across the polymeric membrane. By applying both theoretical [34][35] and empirical [19] relationships from the literature to evaluate the water flow rate crossing the CCM, it was found that the term $\dot{V}_{H_2O,cross}$ is negligible compared to the chosen value of water entering the cathode (which is 0.15 LPM) for all the analyzed electrolyser operating conditions. The outlet flow of water can be thus approximated, considering it equal to the inlet without losing accuracy in the computation of the FRR.

Figure 6 shows the averaged outlet F^- ions concentration and the related derived cathodic area specific FRR for the various CCMs at 60°C (Figure 6a) and 80°C (Figure 6b) with values computed as an average of the last three IC measurements. As shown in Figure 6a, a clear difference in FRR between the two Nafion 117 CCMs and the thinner Nafion 212 exists. The Nafion 117-based CCMs are characterized by quite similar values of FRR_A in the investigated current density range except for the values at 0.2 A/cm^2 where a more relevant difference is observed. The thinner CCM presents instead much lower FRR_A values with respect to the thicker membranes. Concerning for example the 60°C case, the Nafion 212- and 117-based cells are characterized by an area specific FRR peak of approximately 0.3 and 1.3-1.4 µg/h/cm^2, respectively. The FRR_A values computed by Fouda-Onana *et al.* [18]

and Chandesris *et al.* [19] are in the same order of magnitude of the ones presented in this study.

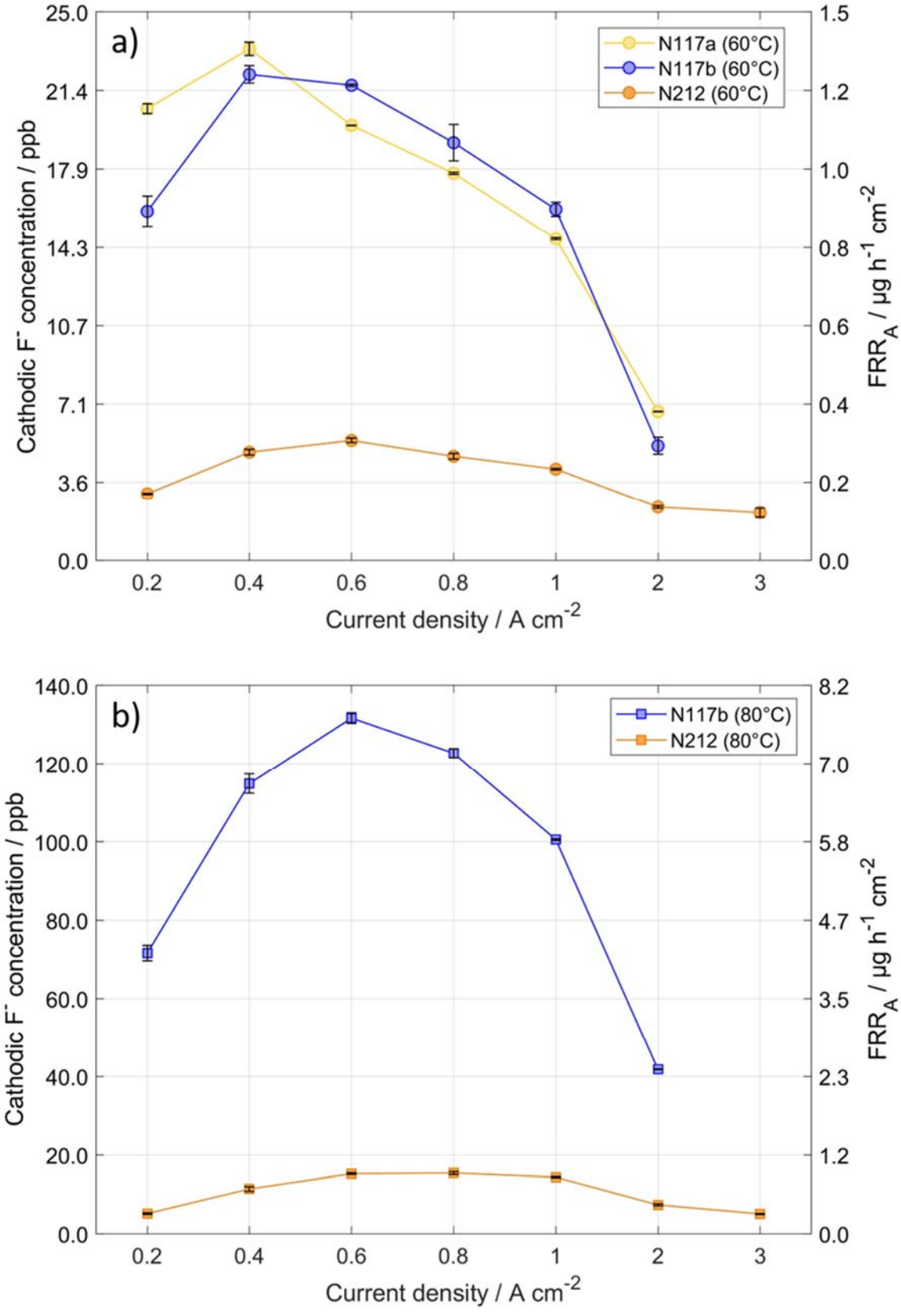

Figure 6. *Cathode outlet concentration (cathodic water flow rate of 0.15 LPM) and area specific FRR at different current densities at 60°C* ***(a)*** *and 80°C* ***(b).***

Another point to consider is that the thin membrane has an equivalent weight (EW) of around 2100 g/mol, which is higher than the one of Nafion 117 CCMs (about 1100 g/mol). Lower EW increases the water uptake of the membrane and generally improves the proton conductivity. However, it may also result in reduced mechanical integrity because of swelling-related issues [36]. Higher EW is thus beneficial for thinner membranes, which are more susceptible to mechanical failure. The differences in EW may also have an effect on the FRR. Rodgers *et al.* [37] observed that the EW of PFSA membranes has a relevant effect on their properties with consequent impact on fuel cell performance and durability, showing that the rate of fluoride emission was approximately 50% lower for a 1100 EW based cell compared to the 950 EW. The increased chemical stability with higher EW was ascribed to a lower concentration of sulfonic acid side chains. The side chain attack by radicals is in fact generally considered as a possible initiation of membrane degradation, resulting in -COOH formation (and subsequent unzipping mechanism, described by reaction 3) [38]. In particular, the C-S bond located at the side chain end was shown to be one of the main targets and the weakest site against hydroxyl radical attack [12][39]. On the other hand, the measured FRR from PEMWEs cannot exclusively be attributed to side chain degradation. Hence, the FRR cannot be expected to be proportional to the EW. Moreover, as previously stated, being the catalyst layer composition the same for the three tested CCMs, its effect was neglected in this comparative analysis. Further research will be addressed to better investigate the role of CL binder and membrane in the release of fluoride ions.

3.5 Fluoride concentration at stack cathode outlet

The aim of the stack measurements is to show that the new online IC measurement methodology is also applicable and feasible for larger commercially available PEM electrolyser systems. The ion chromatography technique using a 850 Professional IC – Anion – MCS - Prep 2 device was connected to the cathode outlet of a 10 cell PEMWE short stack. The performance of the stack was analysed by carrying out polarization curves at different operating conditions. Figure 7a shows the polarization curves at ambient pressure and at three different temperatures (35, 50 and 60 °C, respectively). The water flow rate at the anode inlet was set to 3 LPM.

For the IC measurements, a small water flow rate of 0.2 LPM was set to recirculate through the cathode circuit. As shown in Figure 7b, the effect of current on the release of fluoride ions was investigated by performing current sensitivity tests in the range 0.2-1.9 A/cm^2, keeping constant each operating condition for 3 hours. The working temperature of 60 °C was set for the test. It can be noticed a peak in the fluoride concentration of 9.5 ppb at around 0.2 A/cm^2. Similarly, to the single cell tests, a cathode conductivity peak is also observed.

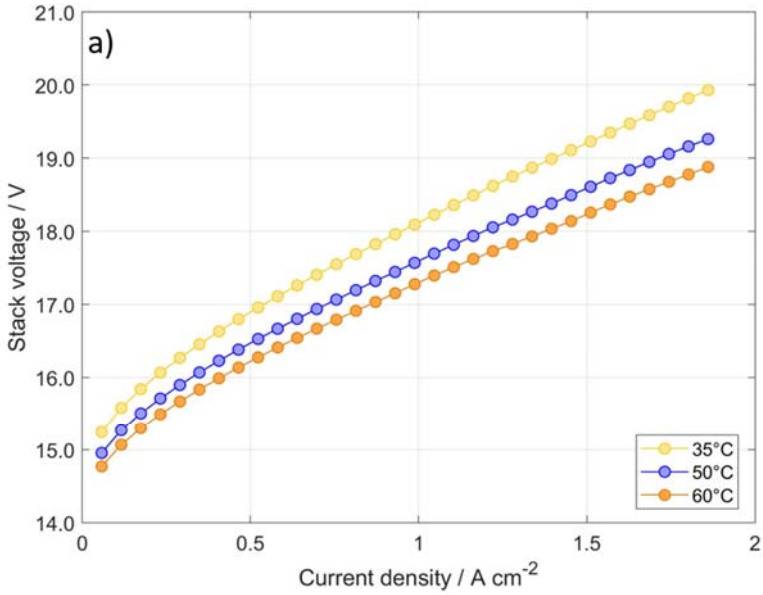
a)
Stack voltage / V
Current density / A cm-2
35°C
50°C
60°C

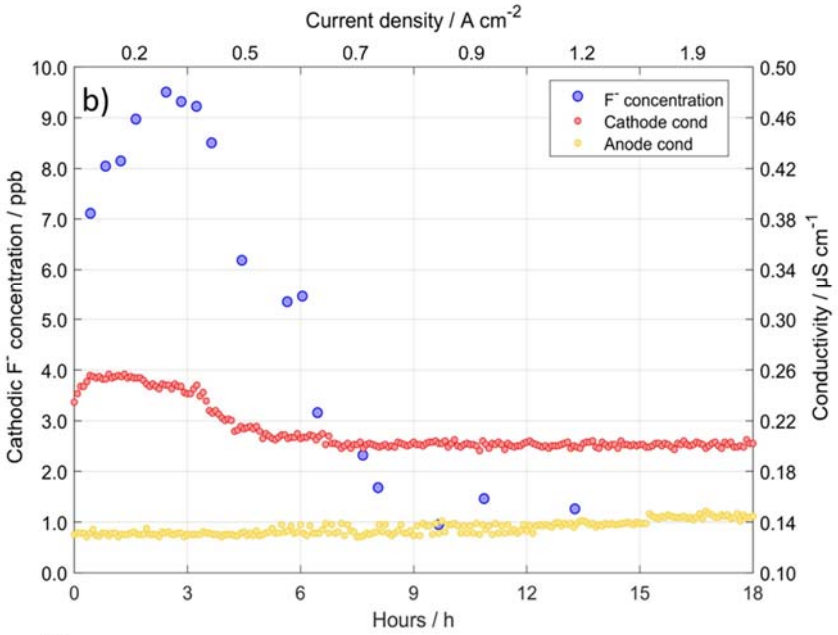
b)
Current density / A cm-2
F- concentration
Cathode cond
Anode cond
Cathodic F- concentration / ppb
Conductivity / µS cm-1
Hours / h

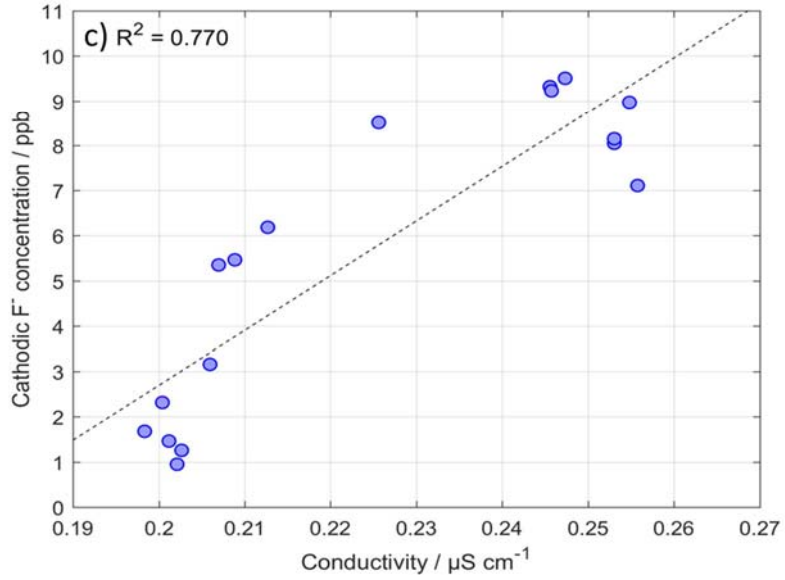
c) R2 = 0.770
Cathodic F- concentration / ppb
Conductivity / µS cm-1

Figure 7. *PEMWE short stack measurements.* ***(a)*** *Polarization curves at ambient pressure, 3 LPM water flow rate at the anode inlet and at 35, 50 and 60 °C,* ***(b)*** *Current sensitivity at 60°C, ambient pressure and water recirculation at the cathode side (0.2 LPM): effect of current density on the fluoride concentration at the cathode outlet and on the cathode water conductivity and* ***(c)*** *Fluoride concentration at the cathode outlet vs. water conductivity at the cathode.*

In order to have an estimation of the FRR, additional IC measurements were performed at the cathode inlet. However, no fluoride concentration was detected in the recirculated water flow, even at low current densities (the highest detected value by the IC device was around 1 ppb). Additionally, an experiment with no cathodic water recirculation (dead-end operation) at 0.2 A/cm^2 was carried out. This measurement resulted in a fluoride concentration of around 23 ppb. This value is higher than the one of Figure 7b, which is approximately 9.5 ppb, since the water stream is less diluted (because no water is recirculated through the cathode). This last test was necessary to quantify the FRR considering the effect of water crossing the membrane. Considering the 0.2 A/cm^2 condition and applying Equations 1 and 2 to both the case with and without water recirculation, it was found the area specific FRR to be around 0.22 µg/h/cm^2/cell. This value is lower compared to what found for the N117 single cells at the same temperature of 60°C (whose FRR in that current density region was around 0.8-1.2 µg/h/cm^2), but still in the same order of magnitude.

The resulting stack FRR value was derived by dividing the total amount of released fluoride by the number of cells composing the stack. However, it cannot be discarded that some cells may deviate from the average FRR values. Analyzing the long term behavior of PEM stacks, Stucki *et al.* [3] found the membrane degradation process (in terms of membrane thinning) to depend on the position of the cell in the electrolyser stack. Inhomogeneities in

current distributions could for example lead to an uneven temperature distribution within the stack. Temperature, as shown in our study from single cells results, has a strong influence on the membrane loss of fluoride. Moreover, it has to be noted that the stack was operated for at least 500 hours before performing those tests, unlike the single cells where the measurements were taken directly after the break-in. This could further contribute in the discrepancy between the obtained stack and single cells results. As an example, in the framework of the NOVEL project [21], a long term durability test was carried out showing a progressive reduction in the detected fluoride release with increasing operating time. Finally, a difference in concentration of metallic ions within the water flow of the single cell and stack system can have a relevant impact on the fluoride release. Chandesris *et al.* [19] for example showed that the degradation rate of the membrane is almost directly proportional to the Fe^{2+} source term.

Nevertheless, analogously to the single cell tests, when performing the current sensitivity experiment, fluoride concentration and cathodic conductivity profiles were observed to have a similar trend. As seen in Figure 7c, an acceptable linear correlation between the two quantities, with a R-squared value of around 0.77 was computed. The water conductivity at the anode side was also shown to have low variation when changing operating condition and to be lower than the one at the cathode in the whole tested operating range. The usage of the online IC monitoring technique was demonstrated to be able to capture the dynamic of change in fluoride release for both single cells and stacks.

4. Conclusions

The online IC measurement methodology developed in this study is shown to be an effective and accurate way to continuously monitor fluoride ion release from PEM electrolyser cells,

allowing to observe transients in fluoride production when changing the electrolyser operating conditions both at single cell and stack level.

Current density and temperature have a considerable effect on FRRs independent of the membrane thickness. PEM electrolysers show high fluoride release rates at low current densities (i.e., 0.4-0.6 A/cm^2) and increased operating temperature, thus potentially inducing an acceleration of the membrane chemical degradation.

The thinner Nafion 212 CCM is characterized by lower area specific FRR values compared to the thicker Nafion 117-based membranes. This lower release of fluoride ions may be ascribed to the higher equivalent weight (solution which is generally preferred for thinner CCMs to improve their mechanical integrity). Thin CCMs seem therefore to have sufficient PFSA membrane chemical stability, with reduced F^- ion emission, to be considered as a potentially viable way to reduce today's PEMWE capital expenditures as long as high hydrogen crossover and safety issues can be avoided.

Finally, a linear correlation between fluoride concentration at the electrolyser outlet and water conductivity at the cathode was found. At single cell level, R^2 was approximately 0.95 and 0.99 for 60°C and 80°C tests, respectively. These two quantities are acceptably correlated at the stack level as well, with a R-squared value of 0.77. This is in accordance with a membrane degradation mechanism involving radical attack and subsequent release of HF molecules, as for example described by the commonly accepted unzipping process. Conductivity is also shown to be much lower in the anode water circuit, in line with CCM chemical attack occurring mainly at the cathode side. Because of this strict correlation between conductivity and fluoride concentration, the measurement of conductivity, using low cost sensors generally found in all PEM electrolysis test systems, could thus represent a practical and low cost indicator for the monitoring of the membrane chemical stability over time.

Acknowledgements

Financial support from the Research Council of Norway, Førny2020 project number 296303, is greatly acknowledged. The Research Council of Norway is also acknowledged for the support to the Norwegian Fuel cell and Hydrogen Centre and the ENERSENSE program.

Nomenclature

Symbols:

A_{cell}	Cell active area	[cm^2]
FRR_A	Area specific fluoride release rate	[µg/h/cm^2]
ppb_F	Fluoride concentration in parts per billion	[-]
R^2	Coefficient of determination	[-]
$\dot{V}_{H_2O}$	Water volume flow rate	[LPM]

Subscripts:

an	PEM cell anode side
cat	PEM cell cathode side
inlet	PEM cell inlet
outlet	PEM cell outlet

Acronyms and abbreviations:

AST	Accelerated Stress Test
BBP	Bipolar Plate
BOL	Beginning Of Life
CCM	Catalyst Coated Membrane
CL	Catalyst Layer
DI	Deionized
EW	Equivalent Weight
FC	Fuel Cell
FRR	Fluoride Release Rate
HER	Hydrogen Evolution Reaction
IC	Ion Chromatography
ISE	Ion Selective Electrode
LEL	Lower Explosion Limit
LPM	Liters Per Minute
MCM	Metrohm CO_2 Suppressor
MEA	Membrane Electrode Assembly
MSM	Metrohm Suppressor Module
OER	Oxygen Evolution Reaction

PEM	Proton Exchange Membrane
PEMFC	Proton Exchange Membrane Fuel Cell
PEMWE	Proton Exchange Membrane Water Electrolysis
PFSA	Perfluorosulfonic acid
PTL	Porous Transport Layer
SEM	Scanning Electron Microscope

References

[1] D. Bessarabov, H. Wang, H. Li, and N. Zhao, *PEM Electrolysis for Hydrogen Production: Principles and Applications*. 2016.

[2] Q. Feng *et al.*, “A review of proton exchange membrane water electrolysis on degradation mechanisms and mitigation strategies,” *J. Power Sources*, vol. 366, pp. 33–55, 2017.

[3] S. Stucki, G. G. Scherer, S. Schlagowski, and E. Fischer, “PEM water electrolysers: Evidence for membrane failure in 100 kW demonstration plants,” *J. Appl. Electrochem.*, vol. 28, no. 10, pp. 1041–1049, 1998.

[4] S. A. Grigoriev, K. A. Dzhus, D. G. Bessarabov, P. Millet, and O. Cedex, “Failure of PEM water electrolysis cells : Case study involving anode dissolution and membrane thinning,” *Int. J. Hydrogen Energy*, vol. 39, no. 35, pp. 20440–20446, 2014.

[5] M. Schalenbach, M. Carmo, D. L. Fritz, J. Mergel, and D. Stolten, “Pressurized PEM water electrolysis: Efficiency and gas crossover,” *Int. J. Hydrogen Energy*, vol. 38, no.

35, pp. 14921–14933, 2013.

[6] P. Trinke, B. Bensmann, and R. Hanke-Rauschenbach, “Experimental evidence of increasing oxygen crossover with increasing current density during PEM water electrolysis,” *Electrochem. commun.*, vol. 82, pp. 98–102, 2017.

[7] H. Liu, F. D. Coms, J. Zhang, H. A. Gasteiger, and A. B. LaConti, *Chemical Degradation: Correlations Between Electrolyzer and Fuel Cell Findings*. 2009.

[8] A. B. LaConti, H. Liu, C. Mittelsteadt, and R. C. McDonald, “Polymer electrolyte membrane degradation mechanisms in fuel cells- findings over the past 30 years and comparison with electrolyzers,” *ECS Trans.*, vol. 1, no. 8, pp. 199–219, 2006.

[9] K. H. Wong and E. Kjeang, “Mitigation of Chemical Membrane Degradation in Fuel Cells : Understanding the Effect of Cell Voltage and Iron Ion Redox Cycle,” *ChemSusChem*, vol. 8, pp. 1072–1082, 2015.

[10] S. Siracusano, N. Van Dijk, R. Backhouse, L. Merlo, and V. Baglio, “Degradation issues of PEM electrolysis MEAs,” *Renew. Energy*, vol. 123, pp. 52–57, 2018.

[11] M. Danilczuk, S. Schlick, and F. D. Coms, “Degradation Mechanism of Perfluorinated Membranes,” in *The Chemistry of Membranes Used in Fuel Cells*, 2018, pp. 19–53.

[12] L. Ghassemzadeh and S. Holdcroft, “Quantifying the Structural Changes of Perfluorosulfonated Acid Ionomer upon Reaction with Hydroxyl Radicals,” *J. Am. Chem. Soc.*, vol. 135, no. 22, pp. 8181–8184, 2013.

[13] T. Xie and C. A. Hayden, “A kinetic model for the chemical degradation of perfluorinated sulfonic acid ionomers : Weak end groups versus side chain cleavage,” *Polymer (Guildf).*, vol. 48, no. 19, pp. 5497–5506, 2007.

[14] M. Pianca, E. Barchiesi, G. Esposto, and S. Radice, “End groups in fluoropolymers,” *J. Fluor. Chem.*, vol. 95, no. 1–2, pp. 71–84, 1999.

[15] H. Monjid, “PEM Electrolyzer Incorporating an Advanced Low Cost Membrane,” 2013.

[16] R. Baldwin, M. Pham, A. Leonida, J. Mcelroy, and T. Nalette, “Hydrogen-oxygen proton-exchange membrane fuel cells and electrolyzers,” *J. Power Sources*, vol. 29, pp. 399–412, 1990.

[17] T. A. Aarhaug, “Assessment of PEMFC Durability by Effluent Analysis,” Norwegian University of Science and Technology, Trondheim, 2011.

[18] F. Fouda-Onana, M. Chandesris, V. Médeau, S. Chelghoum, D. Thoby, and N. Guillet, “Investigation on the degradation of MEAs for PEM water electrolysers part I: Effects of testing conditions on MEA performances and membrane properties,” *Int. J. Hydrogen Energy*, vol. 41, no. 38, pp. 16627–16636, 2016.

[19] M. Chandesris, V. Medeau, N. Guillet, S. Chelghoum, D. Thoby, and F. Fouda-Onana, “Membrane degradation in PEM water electrolyzer : Numerical modeling and experimental evidence of the influence of temperature and current density,” *Int. J. Hydrogen Energy*, vol. 40, no. 3, pp. 1353–1366, 2015.

[20] S. H. Frensch *et al.*, “Impact of iron and hydrogen peroxide on membrane degradation for polymer electrolyte membrane water electrolysis : Computational and experimental investigation on fluoride emission,” *J. Power Sources*, vol. 420, pp. 54–62, 2019.

[21] NOVEL, “NOVEL project.” [Online]. Available: https://www.sintef.no/projectweb/novel/. [Accessed: 15-Apr-2020].

[22] H. Wang, Y. Xiao-Zi, and H. Li, *PEM fuel cell diagnostic tools*. CRC Press, Taylor &

Francis Group, Boca Raton, Florida, 2012.

[23] U. Babic, M. Suermann, F. N. Büchi, L. Gubler, and T. J. Schmidt, “Review - Identifying critical gaps for polymer electrolyte water electrolysis development,” *J. Electrochem. Soc.*, vol. 164, no. 4, pp. F387–F399, 2017.

[24] T. Malkow, A. Pilenga, and G. Tsotridis, *EU Harmonised Polarisation Curve Test Method for Low Temperature Water Electrolysis*. 2018.

[25] “Norwegian Fuel Cell and Hydrogen Centre.” [Online]. Available: https://www.sintef.no/projectweb/nfch/. [Accessed: 29-Jun-2020].

[26] M. J. Kelly, G. Fafilek, J. O. Besenhard, H. Kronberger, and G. E. Nauer, “Contaminant absorption and conductivity in polymer electrolyte membranes,” *J. Power Sources*, vol. 145, pp. 249–252, 2005.

[27] S. Sun, Z. Shao, H. Yu, G. Li, and B. Yi, “Investigations on degradation of the long-term proton exchange membrane water electrolysis stack,” *J. Power Sources*, vol. 267, pp. 515–520, 2014.

[28] S. A. Grigoriev, D. G. Bessarabov, A. S. Grigoriev, N. V Kuleshov, and V. N. Fateev, “On the contamination of membrane-electrode assemblies of water electrolysers based on proton exchange membrane in the course of operation,” *Bulg. Chem. Commun.*, vol. 50, no. Special Issue A, pp. 102–107, 2018.

[29] V. A. Sethuraman, J. W. Weidner, A. T. Haug, S. Motupally, and L. V. Protsailo, “Hydrogen Peroxide Formation Rates in a PEMFC Anode and Cathode,” *J. Electrochem. Soc.*, vol. 155, no. 1, p. B50, 2008.

[30] V. A. Sethuraman, J. W. Weidner, A. T. Haug, M. Pemberton, and L. V. Protsailo,

"Importance of catalyst stability vis-à-vis hydrogen peroxide formation rates in PEM fuel cell electrodes," *Electrochim. Acta*, vol. 54, no. 23, pp. 5571–5582, 2009.

[31] A. Pozio, R. F. Sil, M. De Francesco, and L. Giorgi, "Nafion degradation in PEFCs from end plate iron contamination," *Electrochim. Act*, vol. 48, no. 11, pp. 1543–1549, 2003.

[32] J. Healy *et al.*, "Aspects of the Chemical Degradation of PFSA Ionomers used in PEM Fuel Cells," *Fuel Cells*, vol. 5, no. 2, pp. 302–308, 2005.

[33] W. J. Hamer and H. J. De Wane, *Electrolytic conductance and the conductances of the Halogen Acids in Water*. 1970.

[34] F. Marangio, M. Santarelli, and M. Calì, "Theoretical model and experimental analysis of a high pressure PEM water electrolyser for hydrogen production," *Int. J. Hydrogen Energy*, vol. 34, no. 3, pp. 1143–1158, 2009.

[35] P. Medina and M. Santarelli, "Analysis of water transport in a high pressure PEM electrolyzer," *Int. J. Hydrogen Energy*, vol. 35, no. 11, pp. 5173–5186, 2010.

[36] F. Barbir, *PEM Fuel Cells. Theory and practice*, 2nd Editio. 2013.

[37] M. P. Rodgers, B. P. Pearman, N. Mohajeri, L. J. Bonville, and D. K. Slattery, "Effect of perfluorosulfonic acid membrane equivalent weight on degradation under accelerated stress conditions," *Electrochim. Acta*, vol. 100, pp. 180–187, 2013.

[38] K. H. Wong and E. Kjeang, "Macroscopic In-Situ Modeling of Chemical Membrane Degradation in Polymer Electrolyte Fuel Cells," *J. Electrochem. Soc.*, vol. 161, no. 9, pp. 823–832, 2014.

[39] M. Kumar and S. J. Paddison, "Side-chain degradation of perfluorosulfonic acid

membranes : An ab initio study,” *J. Mater. Res.*, vol. 27, no. 15, pp. 1982–1991, 2012.